

# Electrical switching of altermagnetism

Yiyuan Chen<sup>†,1,2</sup> Xiaoxiong Liu<sup>†,1,2</sup> Hai-Zhou Lu,<sup>1,2,\*</sup> and X. C. Xie<sup>3,4,5</sup>

<sup>1</sup>Department of Physics and Guangdong Basic Research Center of Excellence for Quantum Science, Southern University of Science and Technology (SUSTech), Shenzhen 518055, China

<sup>2</sup>Quantum Science Center for Guangdong-Hong Kong-Macao Greater Bay Area (Guangdong), Shenzhen 518045, China

<sup>3</sup>International Center for Quantum Materials, School of Physics, Peking University, Beijing 100871, China

<sup>4</sup>Institute for Nanoelectronic Devices and Quantum Computing, Fudan University, Shanghai 200433, China

<sup>5</sup>Hefei National Laboratory, Hefei 230088, China

Switching magnetism using only electricity is of great significance for information applications but remains challenging. We find that, altermagnetism, as a newly discovered unconventional magnetism, may open an avenue along this effort. Specifically, to have deterministic switching, i.e., reversing current direction must reverse magnetic structure, parity symmetry has to be broken. We discover that due to their symmetry that depends on chemical environments, altermagnet devices may naturally carry the parity symmetry breaking required for deterministic electrical switching of magnetism. More importantly, we identify MnTe and FeS bilayers as candidate devices. This scheme will inspire further explorations on unconventional magnetism and potential applications.

**Introduction** - Magnetic materials have been a focal point in condensed matter physics and materials science, brewing diverse applications in technology, energy storage, and sensing. While ferromagnetic materials are well applied, antiferromagnetic materials offer advantages like quicker dynamics and resilience to external magnetic fields [1–5]. Recently, there has been increasing interest in altermagnetism, a new category of collinear antiferromagnetic phase, offering unique properties and potential applications [6–9]. The symmetry of altermagnets is determined not only by the magnetic moments but also the chemical environments (Fig. 1), dictated by spin space groups [10, 11]. Their rotation-related sublattices with opposite magnetic moments breaks time reversal symmetry, holding the potential to exhibit other ferromagnetic features such as anomalous Hall effect [12–21], which offers a better readout signal in information storage, compared to the previous antiferromagnets. On the other hand, using pure electrical methods to switch magnetism is a long-standing goal for facilitating applications, but switching altermagnetism still relies on magnetic fields [22], which is highly unfavorable. The mechanism of pure electrical switching of altermagnetism remains an open question.

In this Letter, we propose a scheme to switch altermagnetism deterministically using a pure electric current. We discover that due to their symmetry that depends on chemical environments, altermagnet devices may naturally carry the parity symmetry breaking required for deterministic electrical switching of magnetism. With a MnTe bilayer as an example, the discovery is verified by a symmetry analysis and first-principles calculations. More importantly, our scheme can be generalized to other altermagnets, to inspire more future explorations.

**Symmetry analysis of deterministic switching** - First of all, parity symmetry breaking is a fundamental symmetry requirement for a magnet to be deterministically switched by a pure electric current, i.e., the magnetic

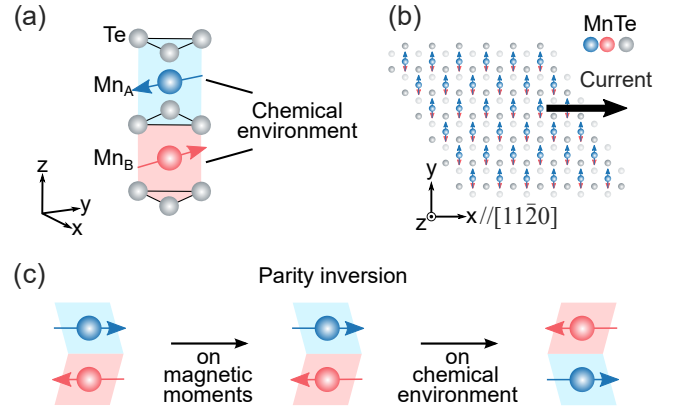


FIG. 1. (a) Crystal and magnetic structures of an altermagnet candidate MnTe. Te atoms around Mn atoms form different chemical environments (cyan and pink shadows). (b) Schematic of the setup for deterministic switching of altermagnetism by a pure electric current (black arrow). Parity symmetry has to be broken in any schemes of all-electric deterministic switching of magnetism, because reversing a current corresponds to applying a parity inversion, under which however a magnetic order remains invariant if the magnet has parity symmetry. (c) When applying parity inversion to a bilayer device of MnTe, the magnetic moments does not change, but the inversion of the chemical environments leads to the broken parity symmetry required for all-electric deterministic switching of altermagnetism.

order has to be reversed when the electric current is reversed. Reversing a current corresponds to applying a parity inversion, under which however a magnetic order remains invariant if the magnet has parity symmetry. In other words, if the magnet has parity symmetry, opposite currents may yield the same magnetic order, which is against the deterministic requirement. Therefore, we need to break parity symmetry.

We will show that parity symmetry can be broken in altermagnet devices due to their symmetry that depends

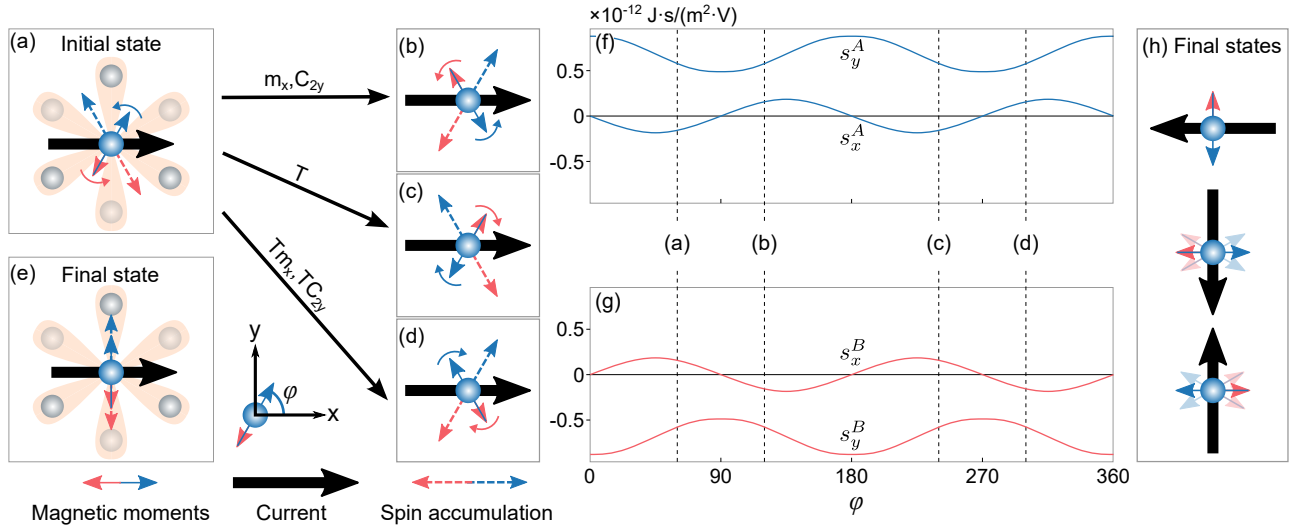


FIG. 2. Microscopic dynamics on why the switching of altermagnetism in a MnTe bilayer by a pure electric current (big black arrow) can be deterministic. (a) An assumed initial state of the Néel order of Mn magnetic moments in the bilayer MnTe. The light yellow shadow indicates six stable positions of the Néel order with a minimal energy, which happen to be aligned with the Te atoms (gray balls). The red and blue solid arrows stand for the magnetic moments of the Mn atoms (red and blue balls). The current can induce spin accumulations (with polarizations indicated by the dashed arrows) on the Mn atoms, depending on the status (measured by the angle  $\varphi$ ) of the Mn magnetic moments. The magnetic moments tend to chase the polarizations of spin accumulation (with the tendency indicated by the curved arrows), resulting the final state of the Néel order in (e) driven by the  $+x$ -direction current. [(b)-(d)] Other possible initial states all have the same tendency to be rotated to the final state in (e), because they can be related to the initial state in (a) by symmetry operations  $m_x, C_{2y}, T, Tm_x, TC_{2y}$ , where  $m_x$  is the mirror reflection with respect to the  $y$ - $z$  plane,  $C_{2y}$  is the two-fold rotation about the  $y$  axis, and  $T$  is time reversal. Therefore, the switching is deterministic, i.e., for the  $+x$ -direction current direction, there is only one final state as shown in (e). [(f) and (g)] The spin accumulations as functions of  $\varphi$  calculated by using Eq. (4) and the density functional theory, with the status of the Mn moments taken into account.  $s_x^A$  means the  $x$ -direction components on Mn atom A, and so on. The dashed lines mark the situations in panels (a), (b), (c), and (d), respectively. [(h)] The final states of the Néel order in the MnTe bilayer tend to be perpendicular to the driving current, as shown for currents along different directions. After turning off the current, the Néel order tends to relax to the nearby stable positions, as shown by the light-color solid arrows.

on chemical environments, to realize the all-electric deterministic switching of altermagnetism. For a specific discussion, we will focus on a promising candidate of altermagnet, MnTe, though our scheme can be generalized to more altermagnets. MnTe has a large spin splitting ( $\sim 370$  meV), high Curie temperature ( $\sim 267$  K) [21], and clear anomalous Hall signal [23]. Te atoms in MnTe form octahedra around Mn atoms, creating different chemical environments (cyan and pink) around the A, B Mn atoms, as shown by Fig. 1(a). The bulk crystal of MnTe has parity symmetry due to the periodic boundary condition in the [0001] crystallographic direction (defined as the  $z$  direction here). To break parity symmetry for deterministic switching as well as to facilitate device applications, we consider a bilayer structure grown along the  $z$  direction.

More importantly, as shown in Fig. 1(c), if the parity inversion is applied only to the magnetic moments of Mn atoms, the magnetic structure remains invariant, but the inversion of the chemical environments gives rise to the broken parity symmetry required for deterministic switching. This is a significant property, showing the

advantage and potential of the MnTe bilayer as well as other altermagnets in pure electrical switching.

*Microscopic dynamics of deterministic switching* - Microscopically, the deterministic switching is guaranteed by the symmetry of the spin accumulations induced by the current. The spin accumulations exert torques to rotate the magnetic moments of the Mn atom. Deterministic switching means that there must be a one-to-one correspondence between the final Néel order and the direction of electric current, no matter the initial Néel order. In addition, the final Néel order has to be aligned with its corresponding spin accumulation, so that the torque vanishes to cease the rotation of the Mn moments.

MnTe has six stable positions for the Néel order, where the energy is minimal [24], as indicated by the shadows in Fig. 2(a). Without loss of generality, we assume a current in the  $x$  direction and a Néel order at an angle  $\varphi$  measured from the  $x$  direction. It is known that the Mn moments in MnTe are always polarized in the  $x$ - $y$  plane [23], so the two Mn moments in the bilayer can always be transformed to each other by a mirror reflection  $m_z$  with respect to the  $x$ - $y$  plane. As a result, the two

Mn moments always have opposite current-induced spin accumulations in the  $x$ - $y$  plane, which lead to the same rotation tendency (as indicated by the curved arrows in Fig. 2) for the two Mn moments and thus a high efficient switching.

We numerically calculate the spin accumulations by using the Kubo formula and first-principles calculations [see from Eqs. (4) through (7)]. Fig. 2(f) and 2(g) show the  $x$  and  $y$  components of the spin accumulations on the A and B Mn atoms, driven by the  $x$ -direction current. According to the calculated results, in Fig. 2(a), for the initial Néel order indicated by the solid arrows, the calculated spin accumulations are indicated as the dashed arrows, which leads to a rotation tendency to the  $y$  directions as indicated by the curved arrows. Roughly speaking, the moments tend to chase the polarization of the spin accumulation, until they are perfectly aligned to stop the rotation. In this way, we show how the  $x$ -direction pure electric current can polarize the Néel order to the  $y$  direction.

More importantly, four types of the initial Néel order can be related to each other by the symmetry operations in Fig. 2(a)-(d), which shows the same rotation tendency towards the  $y$  direction as long as the current is along the  $x$  direction, no matter where the initial Néel order is. Therefore, the microscopic dynamics also shows the deterministic switching of the bilayer altermagnet MnTe using a pure electric current.

Specifically, there are three classes of symmetry operations that transform the Néel order while keeping the crystal structure unchanged. (i) By applying the mirror reflection  $m_x$  with respect to the  $y$ - $z$  plane or two-fold rotation  $C_{2y}$  about the  $y$  axis, the Néel order can be transformed from  $\varphi$  in Fig. 2(a) to  $-\varphi$  in Fig. 2(b). Under these symmetry transformations, the current-induced spin accumulations transform as

$$\begin{aligned} m_x, C_{2y} : \varphi &\rightarrow -\varphi, \\ s_x^{A,B}(\varphi) &= -s_x^{A,B}(-\varphi), \\ s_y^{A,B}(\varphi) &= s_y^{A,B}(-\varphi), \end{aligned} \quad (1)$$

as shown by the calculated results in Figs. 2(f) and 2(g). Therefore, we find that Néel order at  $-\varphi$  angle rotates anticlockwisely under the influence of current-induced spin accumulations. (ii) By applying the time reversal  $T$ , the Néel order can be transformed from  $\varphi$  in Fig. 2(a) to  $\pi + \varphi$  in Fig. 2(c). Under these symmetry transformations, the current-induced spin accumulations transform as

$$\begin{aligned} T : \varphi &\rightarrow \pi + \varphi, \\ s_x^{A,B}(\varphi) &= s_x^{A,B}(\pi + \varphi), \\ s_y^{A,B}(\varphi) &= s_y^{A,B}(\pi + \varphi), \end{aligned} \quad (2)$$

as shown by the calculated results in Figs. 2(f) and 2(g). Therefore, we find that Néel order at  $-\varphi$  angle rotates clockwise under the influence of current-induced spin

accumulations. (iii) By applying  $Tm_x$  or  $TC_{2y}$  about the  $y$  axis, the Néel order can be transformed from  $\varphi$  in Fig. 2(a) to  $\pi - \varphi$  in Fig. 2(b). Under these symmetry transformations, the current-induced spin accumulations transform as

$$\begin{aligned} Tm_x, TC_{2y} : \varphi &\rightarrow \pi - \varphi, \\ s_x^{A,B}(\varphi) &= -s_x^{A,B}(\pi - \varphi), \\ s_y^{A,B}(\varphi) &= s_y^{A,B}(\pi - \varphi), \end{aligned} \quad (3)$$

as shown by the calculated results in Fig. 2(f) and 2(g). Therefore, we find that Néel order at  $\pi - \varphi$  angle rotates clockwise under the influence of current-induced spin accumulations. By summarizing the above analysis, we conclude that the electric current in the  $x$  direction will deterministically switch the Néel order to  $\varphi = \pi/2$ .

Similarly, we can also calculate the spin accumulations generated by the current in the  $y$  direction. Figs. 2(e) and 2(h) show the switching results for current in the  $\pm x$  and  $\pm y$  directions, respectively. The currents in the  $\pm y$  direction switches the Néel order to the middle of two stable positions. The magnetic structure will randomly relax to one of the two nearby stable positions after the current is turned off. The two nearby stable positions, however, have opposite anomalous Hall signal [23], leading to a failure of  $180^\circ$  switching if the current is in the  $\pm y$  directions. Therefore, to achieve a deterministic  $180^\circ$  switching of altermagnetism in the bilayer MnTe, the current should be injected in the  $x \parallel [1\bar{1}\bar{2}0]$  direction.

*Calculation of spin accumulations* - Now we introduce how to calculate the spin accumulations in Fig. 2(f) and 2(g). We calculate the  $i$  component of current-induced spin accumulations on  $a \in \{A, B\}$  Mn atom, by applying the first-principles calculations to the Kubo formula [34, 35]

$$s_i^a = \frac{e\hbar}{2V}\tau \sum_{\nu, \mathbf{k}} \frac{\partial f_\nu}{\partial \epsilon_\nu} (\mathbf{E} \cdot \mathbf{v}_\nu) (\sigma_i^a)_\nu, \quad (4)$$

where  $e$  is the elementary charge,  $\hbar$  is the reduced Planck constant,  $V$  is the volume of the system,  $\tau$  is the relaxation time,  $f_\nu = 1/\{\exp[(\epsilon_\nu - E_F)/k_B T] + 1\}$  is the Fermi-Dirac distribution function,  $\epsilon_\nu$  is the eigen energy of eigen state  $|\nu\rangle$ , the electric field  $\mathbf{E}$  can be converted from the input current density  $\mathbf{j} = \sigma \mathbf{E}$ ,  $\sigma$  is the conductivity,  $\mathbf{v}_\nu = (1/\hbar)\partial \epsilon_\nu / \partial \mathbf{k}$  is the group velocity of eigen state  $|\nu\rangle$ ,  $(\sigma_i^a)_\nu = \langle \nu | \sigma_i^a | \nu \rangle$ ,  $\sigma_i^a = I_a \otimes \sigma_i$  is the local spin accumulation operator on Mn atom  $a$ ,  $I_a$  is an identity matrix with only nonzero element at orbitals of atom  $a$ , and  $\sigma_i = \sigma_{x,y,z}$  are the Pauli matrices.

To evaluate the spin accumulations in the MnTe bilayer accurately, we employ the Wannier interpolation scheme [36, 37] based on the *ab initio* disentangled Wannier functions. The Wannier Hamiltonian reads

$$\mathcal{H}_{a\alpha, b\beta}^W(\mathbf{R}) = \langle 0a\alpha | \hat{\mathcal{H}} | \mathbf{R}b\beta \rangle, \quad (5)$$

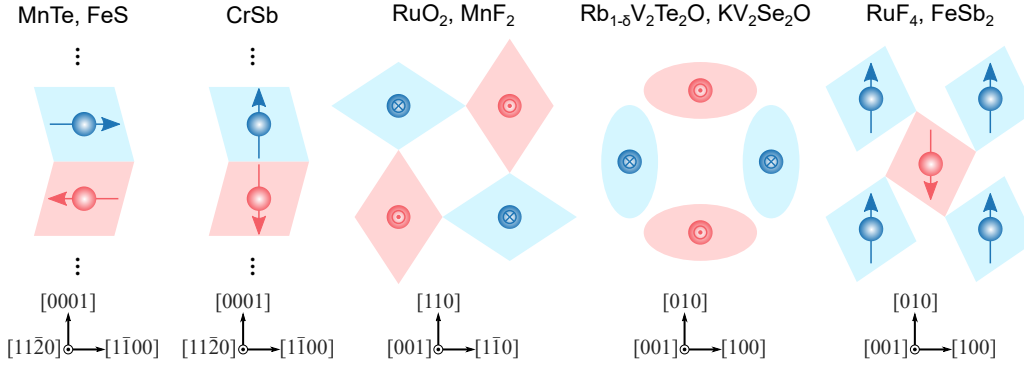


FIG. 3. Symmetry analysis of whether the material candidates for altermagnets can be deterministically switched by pure electric currents, including FeS [25], CrSb [19, 26], RuO<sub>2</sub> [11, 27–29], Rb<sub>1- $\delta$</sub> V<sub>2</sub>Te<sub>2</sub>O [30], KV<sub>2</sub>Se<sub>2</sub>O [31], FeSb<sub>2</sub> [32] and RuF<sub>4</sub> [33]. The arrowed balls indicate the magnetic atoms and the cyan and pink shadows show the chemical environments created by surrounding non-magnetic atoms. Unfortunately, by far most predicted altermagnets have parity symmetry so that they cannot be switched by pure electric currents. FeS, on the other hand, has the same symmetry as that of MnTe, so it also probably can be switched. CrSb, although has the broken parity symmetry, cannot be switched by currents on the plane normal to the [0001] crystallographic direction, due to its Néel order along the [0001] direction.

describing the hoppings from localized orthonormal Wannier function  $|\mathbf{R}b\beta\rangle$  ( $\beta$  orbital of atom  $b$  at lattice  $\mathbf{R}$ ) to  $|\mathbf{0}a\alpha\rangle$  ( $\alpha$  orbital of atom  $a$  at home unit cell  $\mathbf{0}$ ). In momentum space, the eigen energies  $\epsilon_\nu$  and eigen vectors  $|\nu\rangle$  can be found from the eigen equation  $\mathcal{H}(\mathbf{k})|\nu\rangle = \epsilon_\nu|\nu\rangle$ , where the Fourier transform of the Wannier Hamiltonian

$$\mathcal{H}(\mathbf{k}) = \sum_{\mathbf{R}} e^{i\mathbf{k}\cdot\mathbf{R}} \mathcal{H}_{a\alpha, b\beta}^W(\mathbf{R}). \quad (6)$$

The electronic structures of MnTe with various directions of the magnetic moments are calculated via density-functional theory in the pseudopotential framework using VASP [38–40]. To freeze the magnetic moment of MnTe in a random direction, we first calculate the collinear spin-polarized scalar-relativistic electronic structure of the antiferromagnetic MnTe bilayer. The charge density in real space  $\rho_{(\mathbf{r})}^0$  is a scalar on a sampling grid. Then, we project the scalar charge density  $\rho_{(\mathbf{r})}^0$  to a vector charge density, following the direction of the magnetic moment,

$$\begin{aligned} \rho_{(\mathbf{r})}^x &= \rho_{(\mathbf{r})}^0 \sin\theta \cos\phi, \\ \rho_{(\mathbf{r})}^y &= \rho_{(\mathbf{r})}^0 \sin\theta \sin\phi, \\ \rho_{(\mathbf{r})}^z &= \rho_{(\mathbf{r})}^0 \cos\theta, \end{aligned} \quad (7)$$

where  $\theta$  and  $\phi$  are the polar and azimuthal angles of the magnetic moment, respectively. The  $\rho_{(\mathbf{r})}^x$ ,  $\rho_{(\mathbf{r})}^y$ , and  $\rho_{(\mathbf{r})}^z$  are well initial guess for the local spin density approximation (LSDA) method to calculate the non-collinear spin-polarized full-relativistic electronic structure of the MnTe bilayer with a random direction of the magnetic moment. The Wannier functions are disentangled from the Kohn-Sham wave functions, using  $s$ ,  $d$  orbitals of Mn and  $p$  orbitals of Te as projections, by employing Wannier90 code package [41]. The spin accumulation of the

MnTe bilayer on the Fermi surface are evaluated by WannierBerri [42].

*Other altermagnet candidates* - Recent studies have been suggesting an increasing number of candidate materials for altermagnets [17–21, 26, 30–33, 43–47], including FeS [25], RuO<sub>2</sub> [11, 27–29], MnTe [17, 18, 21], CrSb [19, 26], Rb<sub>1- $\delta$</sub> V<sub>2</sub>Te<sub>2</sub>O [30], KV<sub>2</sub>Se<sub>2</sub>O [31] and RuF<sub>4</sub> [33]. Most of the altermagnet candidates are parity symmetric and thus can not be deterministically switched by a pure current, as shown in Fig. 3. To discover the altermagnetic materials that can be electrically switched, we should aim for the materials with parity symmetry broken, e.g., a bilayer MnTe as we study in this work. Nevertheless, parity symmetry breaking is just a necessary requirement. For example, a bilayer CrSb has no parity symmetry, but the easy axis of its Néel order is in the crystallographic [0001] direction, as shown in Fig. 3. Following the symmetry analysis in Fig. 2, currents on the plane normal to the [0001] direction cannot switch the Néel order of the CrSb bilayer between  $\pm[0001]$  directions.

We thank fruitful discussions with Qihang Liu and Chang Liu. This work was supported by the National Key R&D Program of China (2022YFA1403700), Innovation Program for Quantum Science and Technology (2021ZD0302400), the National Natural Science Foundation of China (11925402 and 12350402), Guangdong province (2020KCXTD001), Guangdong Basic and Applied Basic Research Foundation (2023B0303000011), Guangdong Provincial Quantum Science Strategic Initiative (GDZX2201001 and GDZX2401001), the Science, Technology and Innovation Commission of Shenzhen Municipality (ZDSYS20190902092905285), and the New Cornerstone Science Foundation through the XPLOER PRIZE. The numerical calculations were supported by

Center for Computational Science and Engineering of SUSTech.

<sup>†</sup>Yiyuan Chen and Xiaoxiong Liu contributed equally.

\* Corresponding author: [luhz@sustech.edu.cn](mailto:luhz@sustech.edu.cn)

- [1] P. Wadley, B. Howells, J. Železný, C. Andrews, V. Hills, R. P. Campion, V. Novák, K. Olejník, F. Maccherozzi, S. S. Dhesi, *et al.*, “Electrical switching of an antiferromagnet”, *Science* **351**, 587 (2016).
- [2] P. Vaidya, S. A. Morley, J. van Tol, Y. Liu, R. Cheng, A. Brataas, D. Lederman, and E. del Barco, “Subterahertz spin pumping from an insulating antiferromagnet”, *Science* **368**, 160 (2020).
- [3] B. G. Park, J. Wunderlich, X. Martí, V. Holý, Y. Kurosaki, M. Yamada, H. Yamamoto, A. Nishide, J. Hayakawa, H. Takahashi, *et al.*, “A spin-valve-like magnetoresistance of an antiferromagnet-based tunnel junction”, *Nature materials* **10**, 347 (2011).
- [4] Y. Y. Wang, C. Song, B. Cui, G. Y. Wang, F. Zeng, and F. Pan, “Room-temperature perpendicular exchange coupling and tunneling anisotropic magnetoresistance in an antiferromagnet-based tunnel junction”, *Phys. Rev. Lett.* **109**, 137201 (2012).
- [5] X. Marti, I. Fina, C. Frontera, J. Liu, P. Wadley, Q. He, R. Paull, J. Clarkson, J. Kudrnovský, I. Turek, *et al.*, “Room-temperature antiferromagnetic memory resistor”, *Nature materials* **13**, 367 (2014).
- [6] S. Hayami, Y. Yanagi, and H. Kusunose, “Momentum-dependent spin splitting by collinear antiferromagnetic ordering”, *Journal of the Physical Society of Japan* **88**, 123702 (2019).
- [7] L.-D. Yuan, Z. Wang, J.-W. Luo, E. I. Rashba, and A. Zunger, “Giant momentum-dependent spin splitting in centrosymmetric low- $Z$  antiferromagnets”, *Phys. Rev. B* **102**, 014422 (2020).
- [8] S. Hayami, Y. Yanagi, and H. Kusunose, “Bottom-up design of spin-split and reshaped electronic band structures in antiferromagnets without spin-orbit coupling: Procedure on the basis of augmented multipoles”, *Phys. Rev. B* **102**, 144441 (2020).
- [9] L. Šmejkal, J. Sinova, and T. Jungwirth, “Emerging research landscape of altermagnetism”, *Phys. Rev. X* **12**, 040501 (2022).
- [10] P. Liu, J. Li, J. Han, X. Wan, and Q. Liu, “Spin-group symmetry in magnetic materials with negligible spin-orbit coupling”, *Phys. Rev. X* **12**, 021016 (2022).
- [11] L. Šmejkal, J. Sinova, and T. Jungwirth, “Beyond conventional ferromagnetism and antiferromagnetism: A phase with nonrelativistic spin and crystal rotation symmetry”, *Phys. Rev. X* **12**, 031042 (2022).
- [12] L. Šmejkal, R. González-Hernández, T. Jungwirth, and J. Sinova, “Crystal time-reversal symmetry breaking and spontaneous Hall effect in collinear antiferromagnets”, *Sci. Adv.* **6**, eaaz8809 (2020).
- [13] R. González-Hernández, L. Šmejkal, K. Výborný, Y. Yahagi, J. Sinova, T. Jungwirth, and J. Železný, “Efficient electrical spin splitter based on nonrelativistic collinear antiferromagnetism”, *Phys. Rev. Lett.* **126**, 127701 (2021).
- [14] M. Naka, S. Hayami, H. Kusunose, Y. Yanagi, Y. Motome, and H. Seo, “Spin current generation in organic antiferromagnets”, *Nat. commun.* **10**, 4305 (2019).
- [15] H.-Y. Ma, M. Hu, N. Li, J. Liu, W. Yao, J.-F. Jia, and J. Liu, “Multifunctional antiferromagnetic materials with giant piezomagnetism and noncollinear spin current”, *Nat. commun.* **12**, 2846 (2021).
- [16] A. Bose, N. J. Schreiber, R. Jain, D.-F. Shao, H. P. Nair, J. Sun, X. S. Zhang, D. A. Muller, E. Y. Tsymlal, D. G. Schlom, *et al.*, “Tilted spin current generated by the collinear antiferromagnet ruthenium dioxide”, *Nat. Electron.* **5**, 267 (2022).
- [17] T. Osumi, S. Souma, T. Aoyama, K. Yamauchi, A. Honma, K. Nakayama, T. Takahashi, K. Ohgushi, and T. Sato, “Observation of a giant band splitting in altermagnetic MnTe”, *Phys. Rev. B* **109**, 115102 (2024).
- [18] J. Krempaský, L. Šmejkal, S. W. D’Souza, M. Hajlaoui, G. Springholz, K. Uhlířová, F. Alarab, P. C. Constantinou, V. Strocov, D. Usanov, *et al.*, “Altermagnetic lifting of Kramers spin degeneracy”, *Nature* **626**, 517 (2024).
- [19] S. Reimers, L. Odenbreit, L. Šmejkal, V. N. Strocov, P. Constantinou, A. B. Hellenes, R. Jaeschke Ubiergo, W. H. Campos, V. K. Bharadwaj, A. Chakraborty, *et al.*, “Direct observation of altermagnetic band splitting in CrSb thin films”, *Nat. Commun.* **15**, 2116 (2024).
- [20] M. Naka, S. Hayami, H. Kusunose, Y. Yanagi, Y. Motome, and H. Seo, “Anomalous Hall effect in  $\kappa$ -type organic antiferromagnets”, *Phys. Rev. B* **102**, 075112 (2020).
- [21] S. Lee, S. Lee, S. Jung, J. Jung, D. Kim, Y. Lee, B. Seok, J. Kim, B. G. Park, L. Šmejkal, *et al.*, “Broken Kramers degeneracy in altermagnetic MnTe”, *Phys. Rev. Lett.* **132**, 036702 (2024).
- [22] L. Han, X. Fu, R. Peng, X. Cheng, J. Dai, L. Liu, Y. Li, Y. Zhang, W. Zhu, H. Bai, *et al.*, “Electrical 180 switching of Néel vector in spin-splitting antiferromagnet”, *Science Advances* **10**, eadn0479 (2024).
- [23] R. D. Gonzalez Betancourt, J. Zubáč, R. Gonzalez-Hernandez, K. Geishendorf, Z. Šobáň, G. Springholz, K. Olejník, L. Šmejkal, J. Sinova, T. Jungwirth, *et al.*, “Spontaneous anomalous Hall effect arising from an unconventional compensated magnetic phase in a semiconductor”, *Phys. Rev. Lett.* **130**, 036702 (2023).
- [24] D. Kriegner, H. Reichlova, J. Grenzer, W. Schmidt, E. Ressouche, J. Godinho, T. Wagner, S. Y. Martin, A. B. Shick, V. V. Volobuev, *et al.*, “Magnetic anisotropy in antiferromagnetic hexagonal MnTe”, *Phys. Rev. B* **96**, 214418 (2017).
- [25] R. Takagi, R. Hirakida, Y. Settai, R. Oiwa, H. Takagi, A. Kitaori, K. Yamauchi, H. Inoue, J.-i. Yamaura, D. Nishio-Hamane, *et al.*, “Spontaneous Hall effect induced by collinear antiferromagnetic order at room temperature”, *Nature Materials* (2024).
- [26] J. Ding, Z. Jiang, X. Chen, Z. Tao, Z. Liu, J. Liu, T. Li, J. Liu, Y. Yang, R. Zhang, *et al.*, “Large band-splitting in  $g$ -wave type altermagnet CrSb”, [arXiv:2405.12687](https://arxiv.org/abs/2405.12687) (2024).
- [27] K.-H. Ahn, A. Hariki, K.-W. Lee, and J. Kuneš, “Antiferromagnetism in RuO<sub>2</sub> as  $d$ -wave Pomeranchuk instability”, *Phys. Rev. B* **99**, 184432 (2019).
- [28] D.-F. Shao, S.-H. Zhang, M. Li, C.-B. Eom, and E. Y. Tsymlal, “Spin-neutral currents for spintronics”, *Nat. Commun.* **12**, 7061 (2021).
- [29] Z. Lin, D. Chen, W. Lu, X. Liang, S. Feng, K. Yamagami, J. Osiecki, M. Leandersson, B. Thiagarajan,

- J. Liu, *et al.*, “Observation of giant spin splitting and d-wave spin texture in room temperature altermagnet RuO<sub>2</sub>”, [arXiv:2402.04995 \(2024\)](#).
- [30] F. Zhang, X. Cheng, Z. Yin, C. Liu, L. Deng, Y. Qiao, Z. Shi, S. Zhang, J. Lin, Z. Liu, *et al.*, “Crystal-symmetry-paired spin-valley locking in a layered room-temperature antiferromagnet”, [arXiv:2407.19555 \(2024\)](#).
- [31] B. Jiang, M. Hu, J. Bai, Z. Song, C. Mu, G. Qu, W. Li, W. Zhu, H. Pi, Z. Wei, *et al.*, “Discovery of a metallic room-temperature d-wave altermagnet KV<sub>2</sub>Se<sub>2</sub>O”, [arXiv:408.00320 \(2024\)](#).
- [32] I. I. Mazin, K. Koepnik, M. D. Johannes, R. González-Hernández, and L. Šmejkal, “Prediction of unconventional magnetism in doped FeSb<sub>2</sub>”, *P. Natl. Acad. Sci. Usa.* **118**, e2108924118 (2021).
- [33] M. Milivojević, M. Orozović, S. Picozzi, M. Gmitra, and S. Stavri, “Interplay of altermagnetism and weak ferromagnetism in two-dimensional RuF<sub>4</sub>”, *2D Mater.* **11**, 035025 (2024).
- [34] G. D. Mahan, *Many-Particle Physics*, Physics of Solids and Liquids (Springer, New York, 2000).
- [35] Y. Chen, Z. Z. Du, H.-Z. Lu, and X. C. Xie, “Intrinsic spin-orbit torque mechanism for deterministic all-electric switching of noncollinear antiferromagnets”, *Phys. Rev. B* **109**, L121115 (2024).
- [36] J. R. Yates, X. Wang, D. Vanderbilt, and I. Souza, “Spectral and Fermi surface properties from Wannier interpolation”, *Phys. Rev. B* **75**, 195121 (2007).
- [37] J. Qiao, J. Zhou, Z. Yuan, and W. Zhao, “Calculation of intrinsic spin Hall conductivity by Wannier interpolation”, *Phys. Rev. B* **98**, 214402 (2018).
- [38] G. Kresse and J. Furthmüller, “Efficiency of ab-initio total energy calculations for metals and semiconductors using a plane-wave basis set”, *Computational materials science* **6**, 15 (1996).
- [39] G. Kresse and D. Joubert, “From ultrasoft pseudopotentials to the projector augmented-wave method”, *Phys. Rev. B* **59**, 1758 (1999).
- [40] G. Kresse and J. Furthmüller, “Efficient iterative schemes for ab initio total-energy calculations using a plane-wave basis set”, *Phys. Rev. B* **54**, 11169 (1996).
- [41] G. Pizzi, V. Vitale, R. Arita, S. Blügel, F. Freimuth, G. Géranton, M. Gibertini, D. Gresch, C. Johnson, T. Koretsune, *et al.*, “Wannier90 as a community code: new features and applications”, *Journal of Physics: Condensed Matter* **32**, 165902 (2020).
- [42] S. S. Tsirkin, “High performance Wannier interpolation of Berry curvature and related quantities with Wannier-Berri code”, *npj Computational Materials* **7**, 1 (2021).
- [43] Y. Guo, H. Liu, O. Janson, I. C. Fulga, J. van den Brink, and J. I. Facio, “Spin-split collinear antiferromagnets: A large-scale ab-initio study”, *Mater. Today Phys.* **32**, 100991 (2023).
- [44] R.-W. Zhang, C. Cui, R. Li, J. Duan, L. Li, Z.-M. Yu, and Y. Yao, “Predictable Gate-Field Control of Spin in Altermagnets with Spin-Layer Coupling”, *Phys. Rev. Lett.* **133**, 056401 (2024).
- [45] López-Moreno, S and Romero, AH and Mejía-López, J and Muñoz, A, “First-principles study of pressure-induced structural phase transitions in MnF<sub>2</sub>”, *Phys. Chem. Chem. Phys.* **18**, 33250 (2016).
- [46] P. Das, V. Leeb, J. Knolle, and M. Knap, “Realizing Altermagnetism in Fermi-Hubbard Models with Ultracold Atoms”, *Phys. Rev. Lett.* **132**, 263402 (2024).
- [47] B. Jiang, M. Hu, J. Bai, Z. Song, C. Mu, G. Qu, W. Li, W. Zhu, H. Pi, Z. Wei, *et al.*, “Discovery of a metallic room-temperature d-wave altermagnet KV<sub>2</sub>Se<sub>2</sub>O”, [arXiv:2408.00320 \(2024\)](#).